The American Journal of Pathology, Vol. 170, No. 2, February 2007

DOI: 10.2353/ajpath.2007.060692

Musculoskeletal Pathology

Hypoxic Adipocytes Pattern Early Heterotopic Bone Formation

Elizabeth Olmsted-Davis,*†‡ Francis H. Gannon,§ Mustafa Ozen,¶ Michael M. Ittmann,¶ Zbigniew Gugala,‖ John A. Hipp,‡ Kevin M. Moran,‡ Christine M. Fouletier-Dilling,* Shannon Schumara-Martin,* Ronald W. Lindsey,‖ Michael H. Heggeness,‡ Malcolm K. Brenner,‡ and Alan R. Davis*†‡

From the Center for Cell and Gene Therapy and the Departments of Pediatrics,† Orthopedic Surgery,‡ and Pathology,¶ Baylor College of Medicine, Houston, Texas; the Department of Orthopedics and Rehabilitation,‖ University of Texas Medical Branch, Galveston, Texas; and the Department of Bone Biology,§ Armed Forces Institute of Pathology, Washington, DC*

The factors contributing to heterotopic ossification, the formation of bone in abnormal soft-tissue locations, are beginning to emerge, but little is known about microenvironmental conditions promoting this often devastating disease. Using a murine model in which endochondral bone formation is triggered in muscle by bone morphogenetic protein 2 (BMP2), we studied changes near the site of injection of BMP2-expressing cells. As early as 24 hours later, brown adipocytes began accumulating in the lesional area. These cells stained positively for pimonidazole and therefore generated hypoxic stress within the target tissue, a prerequisite for the differentiation of stem cells to chondrocytes and subsequent heterotopic bone formation. We propose that aberrant expression of BMPs in soft tissue stimulates production of brown adipocytes, which drive the early steps of heterotopic endochondral ossification by lowering oxygen tension in adjacent tissue, creating the correct environment for chondrogenesis. Results in *misty* gray lean mutant mice not producing brown fat suggest that white adipocytes convert into fat-oxidizing cells when brown adipocytes are unavailable, providing a compensatory mechanism for generation of a hypoxic microenvironment. Manipulation of the transcriptional control of adipocyte fate in local soft-tissue environments may offer a means to prevent or treat development of bone in extraskeletal sites. ***(Am J Pathol 2007, 170:620–632; DOI: 10.2353/ajpath.2007.060692)***

Heterotopic ossification, defined as the formation of bone in abnormal anatomical locations, can be clinically insignificant or devastating, depending on the site and duration of new bone formation.[1] Besides its high morbidity in total joint arthroplasty, there are many additional causes of heterotopic ossification, including soft-tissue trauma, central nervous system injury, vasculopathies, arthropathies, and inheritance. Fibrodysplasia ossificans progressiva is a rare genetic disorder in which disabling ectopic ossification progresses in a typical anatomical pattern until most or all major joints of the axial and appendicular skeleton are affected[2]; it has recently been found to be attributable to a mutation in ACVRI.[3] Arterial ossification and cardiac valve ossification seem to be highly regulated processes, possibly mediated by bone morphogenetic proteins (BMPs).[4]

Attempts to prevent or treat aberrant bone formation have been restricted by the complexity and multiple causes of the disorder. Nonetheless, new therapies are being devised to target the inductive molecules that may trigger the process, the participating progenitor cells, and local tissue environments conducive to osteogenesis.[1] Gene therapy with BMP antagonists seems especially promising because overexpression of BMP4 and underexpression of physiological BMP antagonists are common findings in some forms of heterotopic ossification.[5] Because angiogenesis is absolutely required for endochondral bone formation and is a prominent feature of embryonic bone formation, fracture callus formation, and the preosseous lesions in fibrodysplasia ossificans progressiva, targeting new blood vessel formation with anti-angiogenic agents may slow or inhibit the production of heterotopic bone.[6]

To gain a more complete understanding of the factors that drive heterotopic ossification, we focused on the microenvironmental conditions needed to induce mesenchymal stem cells to differentiate to chondrocytes, which form the cartilaginous matrix essential to osteoblast recruitment and normal osteoid mineralization during endo-

Supported by the Department of Defense (grants PR0 33166 to E.O.D. and PR0 33169 to A.R.D.).

Accepted for publication October 24, 2006.

Address reprint requests to Alan R. Davis, Baylor College of Medicine, One Baylor Plaza, Houston, TX 77030. E-mail: ardavis@bcm.tmc.edu.

chondral bone formation. Several studies suggest that low oxygen tension critically influences chondrocyte differentiation by accelerating the growth of mesenchymal stem cells and promoting their commitment to the chondrocyte lineage, in part by up-regulating a program of chondrocyte-specific gene expression under the control of hypoxia-inducible factor 1 (HIF-1).[7–9] Although the requirement for low oxygen tension during the initial stages of endochondral bone formation is well accepted, the source of hypoxia in local tissue environments remains primarily undefined.

To address this issue, we relied on a model of heterotopic ossification[10] in which human fibroblasts are transduced to express BMP2 and are then injected into a hind-leg muscle of non-obese diabetic/severe combined immunodeficient (NOD/SCID) mice.[11,12] Heterotopic ossification is induced by a single injection of 5×10^6 fibroblasts (the MRC-5 human line transduced with Ad535 BMP2 or the MC3T3 mouse line transduced with Ad5 BMP2) into the quadriceps or soleus muscle of 6-week-old NOD/SCID mice[11,13] or C57BL/6 mice.[14] We have shown previously,[12] by tracking human cells with an antibody against a mitochondrial protein not cross reactive with mouse, that the injected cells are gone by day 5 and are not directly incorporated into any structure at any stage of heterotopic bone formation. In those studies, we demonstrated that each intermediate structure (eg, cartilage) in the endochondral process that forms heterotopic bone as well as the final heterotopic bone itself consists entirely of cells derived from the host. In addition, we found that the nature of the cells used to produce BMP2 is irrelevant and that many different cell types (eg, lung, skin) can be used, the only relevant parameter being high-level BMP2 production. These findings also strongly support our conclusion that the injected cells serve only as factories for BMP2 production and nothing more. We have relied on this model rather than the use of purified BMP2 because of the known difficulties[15] with this procedure, which include the requirement for large amounts of purified BMP2, short half-life of the BMP2, and the necessity of using a carrier, some of which (eg, Matrigel) have biological activity of their own. The local concentration of BMP2 in these studies is difficult to assess *in vivo*. We have previously published the kinetics of BMP2 production *in vitro.*[11,12] We are currently trying to better assess the activity of BMP2 *in vivo* by staining cells with an antibody against phosphorylated SMAD that marks the response to BMP2.

BMP2 has been used extensively to induce bone formation in patients[16] and differs from BMP4, a candidate inducer of heterotopic ossification,[17] by only a single amino acid change (valine instead of alanine at position 152). Preliminary analysis of the tissue changes within the lesional area suggested that BMP2 released by the transduced fibroblasts recruits and stimulates mesenchymal elements to form mature marrow-containing bone (see Figure 1). This model seems highly relevant to ectopic bone formation in humans because it relies on a BMP molecule that is virtually identical to BMP4 to stimulate endochondral bone formation in extraskeletal muscle. Indeed, both loss-of-function and gain-of-function studies have demonstrated the necessity and sufficiency of BMP2 and BMP4 in regulating the development of cartilage and bone.[18]

In the studies below, we describe the generation of a hypoxic microenvironment critical for heterotopic bone formation and the adipocytes responsible for its generation. We do not address the nature of the stem cells involved in the process, although there are several possibilities. These include muscle satellite cells,[19] bone marrow-derived stem cells,[20,21] and other types of stem cells.[22]

Materials and Methods

Viral Vectors and Cells

An Ad5 vector carrying an adenovirus type-35 fiber and a cDNA for *BMP2* in the E1 region (Ad5F35-BMP2) was constructed, propagated, and purified as previously described.[11,12] The control vector was Ad5F35-HM4, which lacks a transgene cassette but otherwise is identical to Ad5F35-BMP2. Ad5BMP2[11] and Ad5empty, an Ad5 vector lacking a transgene, were also used. MRC-5 human cells, a fetal lung diploid cell that undergoes 60 to 70 population doublings before senescence, was transduced with Ad5F35-BMP2 and injected into NOD/SCID mice. The Ad5-BMP2 vector was used to transduce the C57BL/6 mouse cell line MC3T3 to diminish immune response in these immunocompetent mice strains and was injected into either C57BL/6 or *misty* mice (C57BLKS/J-m; Jackson Laboratories, Bar Harbor, ME). Brown fat is completely absent from all expected locations in *misty* mice.[23] This property was verified by staining for UCP-1, which was uniformly absent from these mice (data not shown).

Adenovirus transductions with Ad5F35 vectors were performed as previously described.[11] MC3T3 cells were transduced with Ad5BMP2 in the presence of Genejammer,[14] a critical procedure for the production of bone in C57BL/6 or *misty* mice. MC3T3 cells lack receptors for both Ad5 (CAR) and Ad5F35 (CD46) and, therefore, Genejammer was used to dramatically increase transduction of these cells.[14] The transduced cells were injected into NOD/SCID, C57BL/6, or *misty* mice as previously described.[11,12] The *misty* mouse is congenic with C57BL/6,[23] and although it completely lacks brown fat,[23] the nature of its genetic defect is unknown. Ad5F35-BMP2 was developed to transduce primary human cells (eg, MSCs, skin fibroblasts, MRC-5), which lack the receptor for Ad5, the coxsackie-adenovirus receptor (CAR), but retain the receptor (CD46) for adenovirus type 35. This vector was used in these studies only when the transduced human cells were to be injected into NOD/SCID mice, in which the immune response is less of a concern.

Ad5 is the standard adenovirus type used by most investigators. To conduct the experiments to compare bone formation in wild-type (C57BL/6) and mutant (*misty* derivative of C57BL/6) mice, we needed to

transduce the cells such that the strong immune response in these immunocompetent mice would be minimized. Ad5BMP2 was used in these studies only to transduce MC3T3 cells for injection of BMP2-expressing murine cells into mice.

Histological Analysis

Decalcified, paraffin-embedded hindlimb (5-μm) sections were prepared by cutting in half the formalin-fixed and decalcified muscle tissue surrounding the site of injection before paraffin embedding and formation of blocks. Sections therefore started from the inner most part of the lesional tissue and continued outward in both directions. After deparaffinization, sections were treated for 5 minutes at room temperature with 0.3% Triton X-100 in Tris-buffered saline (19.98 mmol/L Tris, 136 mmol/L NaCl, pH 7.4), followed by a 10-minute treatment at 37°C with Digest-All 1 (Zymed, San Francisco, CA). When sections were stained using horseradish peroxidase, they were treated for 15 minutes at room temperature with peroxide block (Signet Laboratories, Detroit, MI). Sections were analyzed with a PowerVision Homo-Mouse IHC kit (ImmunoVision Technologies, Daly City, CA), according to the manufacturer's instructions. Both primary and secondary antibodies were bound for 30 minutes at room temperature. For double-antibody labeling, samples were treated simultaneously with the two primary antibodies followed by washing and simultaneous incubation with secondary antibodies, used at 1:000 dilution, to which either Alexa Fluor 488 (green) or Q-dot 525 (green) and Alexa Fluor 647 (red) or Q-dot 580 (red) had been conjugated. In experiments with mouse monoclonal antibodies, we used a Mouse on Mouse kit (Vector Laboratories, Burlingame, CA) and diluted both primary and secondary antibodies in mouse diluents according to the kit instructions except that in immunofluorescence experiments we omitted peroxidase and biotin/avidin blocking and detection of horseradish peroxidase. Primary antibodies to UCP-1 (rabbit polyclonal used at 1:1000 dilution; Chemicon, Temecula, CA), PGC-1α (mouse monoclonal used at 1:500 dilution; Chemicon), von Willebrand factor (rabbit polyclonal used at 1:200 dilution; Chemicon), and S-100 (rabbit polyclonal used at 1:3000 dilution; DAKO, Carpinteria, CA) were used. Horseradish peroxidase-conjugated secondary antibodies, either anti-rabbit or anti-mouse, were part of the PowerVision Homo-Mouse IHC kit and were used without dilution according to the instructions in the kit. Pimonidazole (Hypoxyprobe) and mouse Hypoxyprobe monoclonal antibody, used at a dilution of 1:500, were obtained as a kit from Chemicon and used according to the instructions. Sections were stained routinely with either hematoxylin and eosin (H&E) as described by the Armed Forces Institute of Pathology[24] or, when developed with 3,3-diaminobenzidine, with hematoxylin alone.

Microcomputed Tomography (Micro-CT)

Specimens were scanned with a micro-CT system (eXplore Locus SP; General Electric, London, ON, Canada) at 14-μm resolution. Bone density was determined with a density calibration phantom. Three-dimensional reconstructions of the region injected with BMP2-producing cells were generated to identify regions of heterotopic ossification. The volume of heterotopic mineralized tissue was then calculated with use of the quantitative bone analysis software provided with the micro-CT system. For this analysis, any tissue with a density greater than 0.26 g/ml hydroxyapatite was considered mineralized tissue. The total volume of heterotopic mineralized tissue was measured for the right and left hind limbs, and the difference in values between the *misty* and C57BL/6 mice was assessed by standard *t*-test analysis.

Histomorphometry

Histomorphometry was performed on H&E-stained slides according to standardized protocols[25] using the OsteoMeasure histomorphometry system (Osteometrics Inc., Atlanta, GA).

Microarray Analysis

RNA from the entire quadriceps muscle injected was isolated by the Trizol method from mice ($n = 4$) on each day for 7 days after injection of transduced MRC-5 cells. The integrity of each RNA was checked by either agarose gel electrophoresis or with an Agilent bioanalyzer (Agilent Technologies, Palo Alto, CA). RNA concentrations were determined spectrophotometrically or with the bioanalyzer. The RNA from each animal was processed separately, the results were averaged, and standard deviations calculated for a given group on any day. Equal amounts of BMP2 and empty vector control RNAs were mixed in microarray hybridization procedures. Labeled cDNA (Cy5, BMP2; Cy3, empty vector control) was hybridized to an Agilent G4120A mouse developmental array containing ~40,000 genes. Slides were scanned either in an Agilent dual-laser DNA microarray scanner or in an Axon 4000A dual-channel scanner (Axon Instruments, Foster City, CA); the data were analyzed with either Agilent feature extraction software and Rosetta Resolver (Rosetta Biosoftware Products, Seattle, WA) or Gene Pix version 3.0 software (Axon Instruments).

Results

Detection of Brown Adipocytes during BMP2-Induced Bone Formation

Four mice per experimental group were euthanized each day for 7 days, their tissues fixed in 10% neutral buffered formalin, and paraffin-embedded sections prepared for immunohistochemical analysis. Bone development in this heterotopic model followed a consistent pattern. Multilocular adipocytes were observed between muscle fibers as early as day 1 after injection (Figure 1a) with nascent

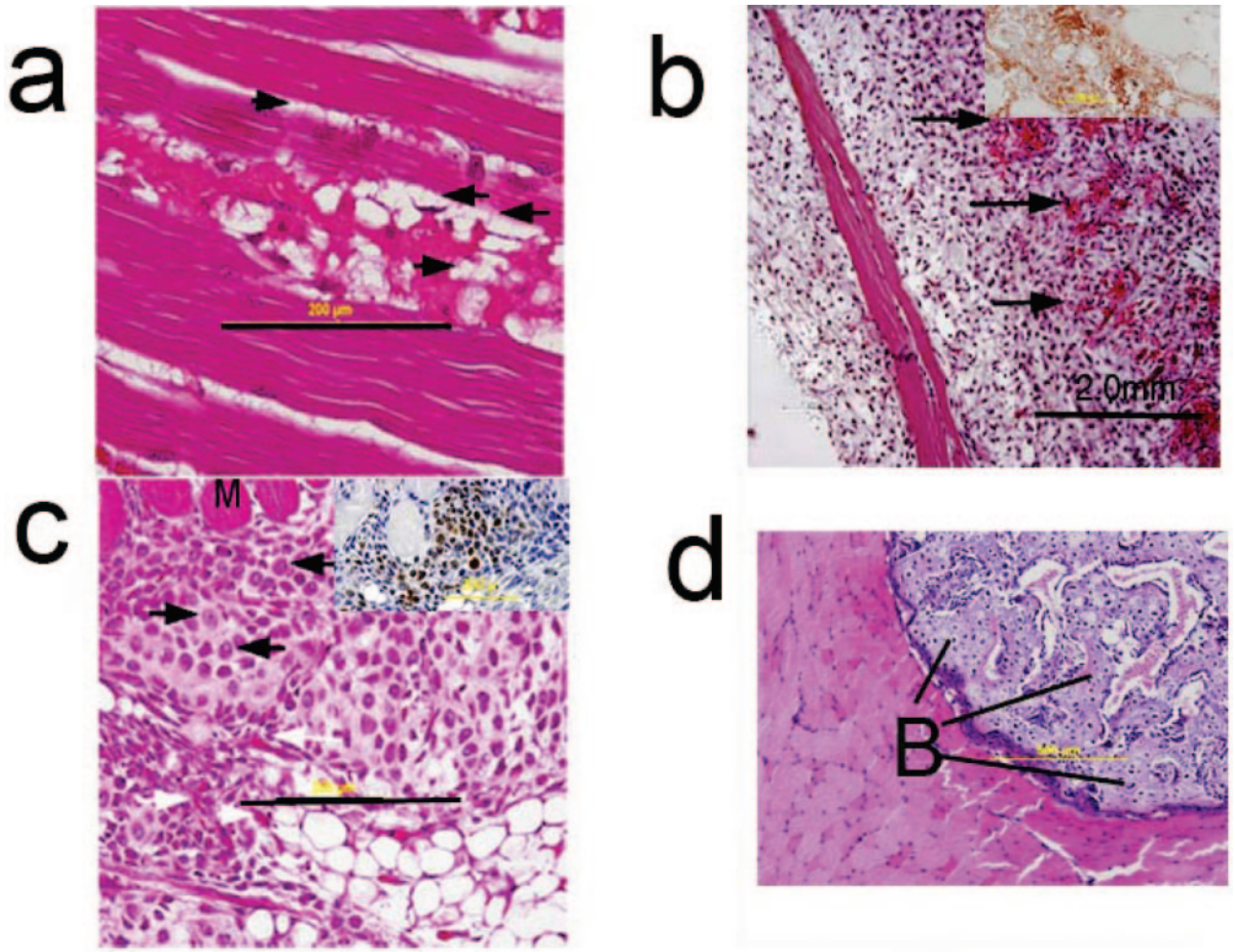

Figure 1. Histological analysis of heterotopic bone formation stimulated by BMP2. **a:** Day 1, cells morphologically similar to brown adipocytes (**arrows**) detected between muscle fibers. **b:** Day 3 or 4, immature vessels (**arrows**) leaking red blood cells (**inset**, VWF staining). **c:** Day 5 or 6, cartilage matrix with embedded chondrocytes [**arrows**; **inset**, S-100 staining; muscle (M)]; **d:** Day 7, bone (B). Original magnifications: ×20.5 (**a**, **c**); ×10.5 (**b**, **d**).

vascularization apparent by 3 or 4 days as indicated by leakage of red blood cells (Figure 1b) or staining with von Willebrand factor (VWF; Figure 1b, inset). Early bone development had progressed to the formation of a cartilaginous matrix with embedded chondrocytes by day 5 or 6 (Figure 1c), clearly evident with typical polygonal morphology and partial staining with Alcian blue (not shown) as well as staining with S-100, a chondrocyte-specific protein (Figure 1c, inset).[26] Mature bone was not evident until 7 days (Figure 1d), although infiltrating adipocytes could not be detected after day 5 or 6.

To characterize further the adipocytes seen on the first day after injection, we used a lipid droplet-specific reagent (Bodipy 493/502; Figure 2, compare a and b) and a reagent that reacts specifically with mitochondria (MitoTracker, Figure 2c). The results show that the smaller brown adipocytes (Figure 2c, yellow arrows), evident only in mice injected with BMP2-producing cells, stain more heavily with this reagent than do the larger white adipocytes. Mice injected with cells transduced with Ad5F35-null produced little or no staining with MitoTracker (Figure 2d). We conclude that the infiltrating adipocytes contained abundant mitochondria in addition to multiple lipid droplets, features common to brown rather than white adipocytes.[27] Importantly, tissues injected with fibroblasts carrying an empty vector lacked multilocular cells altogether (eg, Figure 3C), indicating that the emergence of adipocytes soon after injection of BMP2-expressing cells is linked to bone morphogenesis. To confirm that the infiltrating multilocular cells were truly brown adipocytes, we tested for the expression of uncoupling protein-1 (UCP-1), a definitive marker of this cell type[28,29] that uncouples the electron transport chain from generation of ATP and uses the energy for heat generation. UCP-1 expression was specifically associated with the multilocular cells interspersed among the muscle fibers of both NOD-SCID (Figure 3A) and C57BL/6 mice (Figure 3B). Such cells were not observed in control mice (Figure 3C) nor were they present in *misty* mice (Figure 3D), which do not produce brown adipose tissue.[23]

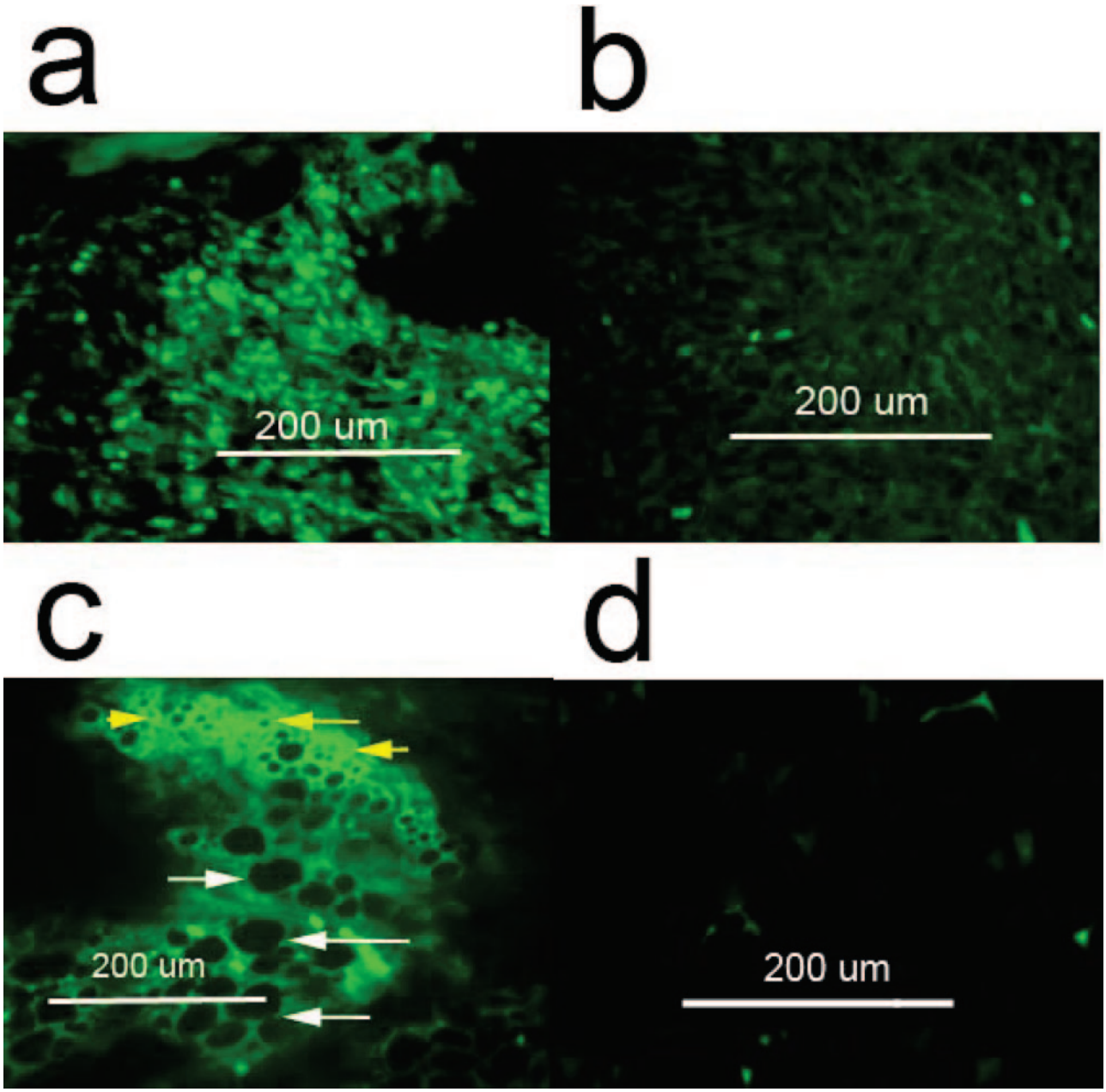

Figure 2. a: Adipocytes recruited after Ad5F35-BMP2 and stained with Bodipy 493/502. **b:** Bodipy staining of muscle injected with cells carrying an empty vector, Ad5F35-null. **c:** Brown (**yellow arrows**) and white (**white arrows**) adipocytes after staining with Mitotracker. **d:** Mitotracker staining of muscle injected with cells carrying an empty vector. Tissues in **a** and **c** were harvested 24 hours after injection of BMP2-producing cells, and those in **b** and **d**, 24 hours after injection of cells transduced with empty vector. Original magnifications, ×20.5.

Genes Involved in Oxygen Consumption Are Up-Regulated

If brown adipocytes truly generate a hypoxic environment, one would expect that the genes involved in energy metabolism, especially those of the mitochondrial electron transport chain, the component that consumes the most molecular oxygen, would be up-regulated. Accordingly, RNA was extracted from the injected quadriceps muscle (n = 4) on each of 7 days after injection of transduced MRC-5 cells. Figure 4A presents the regulation of genes, derived by microarray analysis, involved in glycolysis, the citric acid cycle, and the electron transport chain on the first 2 days after injection of BMP2-producing cells. The numbers are presented as a ratio of the amount of gene-specific RNA produced after injection of BMP2-producing cells to the amount of the same gene-specific RNA produced after injection of cells transduced with empty vector. There was a 42 ± 2-fold induction of phosphofructokinase on day 1. This enzyme converts fructose-6-phosphate to fructose-1,6-bisphosphate, a key step because of its irreversible nature in the glyco-

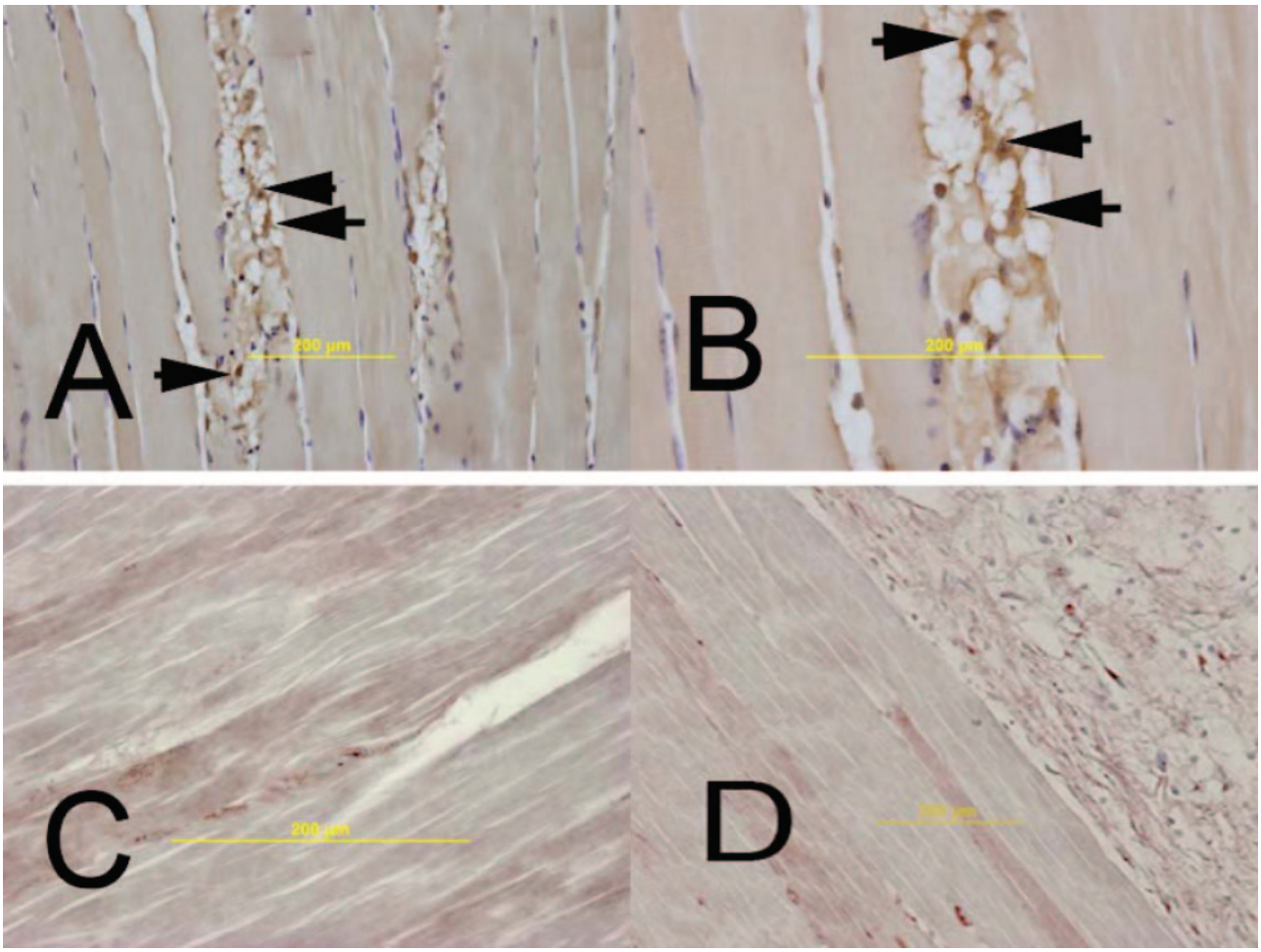

Figure 3. Multilocular adipocytes observed after injection of BMP2-producing cells express UCP-1, a unique marker of brown adipocytes. Staining with antibodies to UCP-1 detected the uncoupling protein (dark brown) on day 2 after stimulation with BMP2 in muscle from both NOD/SCID mice (**A**) and C57BL/6 mice (**B**) but not in muscle stimulated with a control vector (Ad5F35-HM4) (**C**) used to transduce MRC-5 cells injected into a NOD-SCID mouse or taken from a *misty* mouse after treatment with MC3T3 cells transduced to express BMP2 (**D**). Original magnifications: ×20.5 (**A**, **D**); ×40.5 (**B**, **C**).

lytic pathway from glucose to pyruvate that supplies acetyl-CoA to the citric acid cycle, which in turn supplies NADH to the electron transport chain. In addition, on day 2, there was an 11 ± 1.7-fold increase in NADH dehydrogenase 3, a component of complex I of the electron transport chain, responsible for pumping protons generated by glycolysis and the citric acid cycle in the mitochondrial matrix into the intermembrane space where ATP synthase converts ADP to ATP with consumption of molecular oxygen. On day 1, there were also significant increases in subunits c, g, and o of ATP synthase itself, as well as an increase in aquaporin 8, which pumps water from the mitochondria.

Figure 4, B and C, diagram the bioenergetics of oxygen consumption contrasting other cell types (Figure 4B) with brown adipocytes (Figure 4C). Glycolysis and the citric acid cycle supply protons to the electron transport chain, which uses them to generate the proton motive force used to make either ATP, when the electron transport chain is coupled (Figure 4B), or heat (Figure 4C), when it is uncoupled from the conversion of molecular oxygen, obtained from the immediate extracellular environment via release from hemoglobin or myoglobin, to water. Brown adipocytes are well suited to deplete oxygen in the microenvironment because they are laden with mitochondria containing UCP-1 in addition to ATP synthase (Figure 4C).

Brown Adipocytes Generate a Hypoxic Microenvironment

Because brown adipocytes contain abundant mitochondria, we reasoned that their increased consumption of oxygen might impose a hypoxic microenvironment conducive to the formation of a cartilaginous matrix.[30] Thus, oxygen tension was assessed at 3 and 4 days after injection by injecting pimonidazole and examining tissues near the injection site for hypoxic areas, using an antibody (Hypoxyprobe monoclonal antibody) against pimonidazole. Adducts of this reagent form with thiol groups in proteins, peptides, and amino acids and hypoxia ($pO_2 < 10$ mm Hg) is required for binding that is not dependent on the presence of specialized redox enzymes such as P450 nitroreductases. Furthermore, wide variations in NADH and NADPH levels do not change the

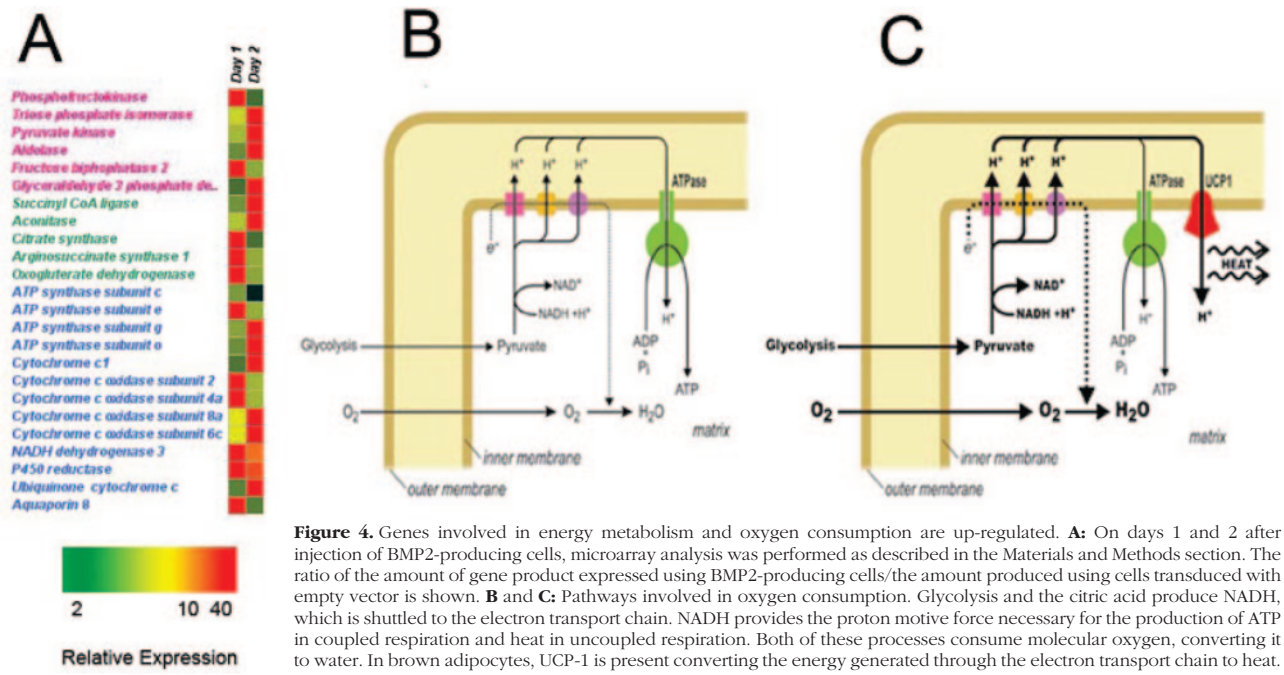

Figure 4. Genes involved in energy metabolism and oxygen consumption are up-regulated. **A:** On days 1 and 2 after injection of BMP2-producing cells, microarray analysis was performed as described in the Materials and Methods section. The ratio of the amount of gene product expressed using BMP2-producing cells/the amount produced using cells transduced with empty vector is shown. **B** and **C:** Pathways involved in oxygen consumption. Glycolysis and the citric acid produce NADH, which is shuttled to the electron transport chain. NADH provides the proton motive force necessary for the production of ATP in coupled respiration and heat in uncoupled respiration. Both of these processes consume molecular oxygen, converting it to water. In brown adipocytes, UCP-1 is present converting the energy generated through the electron transport chain to heat.

oxygen dependence of binding. Figure 5Aa shows large discrete areas of oxygen deficiency in tissue samples from mice receiving cells transduced with Ad5F35 BMP2 for 3 days, in contrast to uniformly normoxic tissues in mice injected with a control vector (Figure 5Ac). As a positive control, we assessed the growth plate in untreated C57BL/6 mice (Figure 5Ab). The hypoxic areas were not difficult to find when scanning slides and always corresponded to areas within the region of heterotopic bone formation and never elsewhere in the tissue. To clarify the origin of these cells, we performed dual labeling with antibodies against pimonidazole and peroxisome proliferator-activated receptor-γ co-activator 1α (PGC-1α), a transcriptional co-activator that regulates genes involved in energy metabolism.[31] Importantly, interaction between PGC-1α and the peroxisome proliferator-activated receptor-γ (PPAR-γ) can activate specific gene expression associated with the conversion of preadipocytes to brown adipocytes.[31] Figure 5A, d–f, shows that the hypoxic cells present in muscle injected with BMP2-secreting cells expressed PCG-1α and therefore were likely newly differentiated brown adipocytes. On days 2 and 3 the hypoxic regions surrounded the brown adipocytes observed between muscle fibers (Figure 5Ba), again indicating the hypoxic nature of these cells. In addition, at later times (day 4), the hypoxic regions occupied a substantial amount of the area of heterotopic ossification (Figure 5Bb). In addition, there was a substantial proportion of the cells that expressed HIF1 (Figure 5Bc) consistent with the substantial up-regulation of several HIF1-dependent proteins such as phosphofructokinase, glyceraldehyde-3-phosphate dehydrogenase, aldolase, and fructose biphosphatase 2 (Figure 4),[32] as well as other pathways linked to HIF1 (E.O.-D., A.R.D., unpublished). These results indicate that the enhanced respiratory activity of brown adipocytes creates a hypoxic microenvironment most likely through the uncoupling of oxidative phosphorylation.[33] This, in turn, would be expected to promote the differentiation of mesenchymal cells to chondrocytes, a necessary step in the formation of a cartilaginous matrix and hence mature bone.[30]

UCP-1 Expression Precedes the Development of Hypoxia, Which Develops in Cells that Contain and Cells that Lack UCP-1

If, indeed, brown adipocytes generate a hypoxic microenvironment, one would expect the development of this cell type to precede the generation of hypoxia. In addition, as oxygen is depleted in the local microenvironment, cells other than brown adipocytes (eg, those lacking UCP-1 expression) should also become hypoxic. To test this prediction, we co-stained sections from mice at 1, 2, 4, and 5 days after injection of BMP2-producing cells (Figure 6, a–d) and injected with pimonidazole for 3 hours, using a rabbit antibody against UCP-1 (green color) and a mouse monoclonal antibody against Hypoxyprobe (red color). The results (Figure 6a) show that UCP-1 is indeed expressed in the absence of hypoxia on day 1. On day 2, one observes some co-expression of UCP-1 with concomitant hypoxia in the same cell (yellow color, Figure 6b) and a substantial amount of UCP-1 in the absence of hypoxia (green color, Figure 6b). However, on days 4 and 5, one observes uniformly hypoxic cells in some regions of the section, either with (Figure 6, c and d; yellow arrows) or without (Figure 6, c and d; red arrows) co-expression of UCP-1.

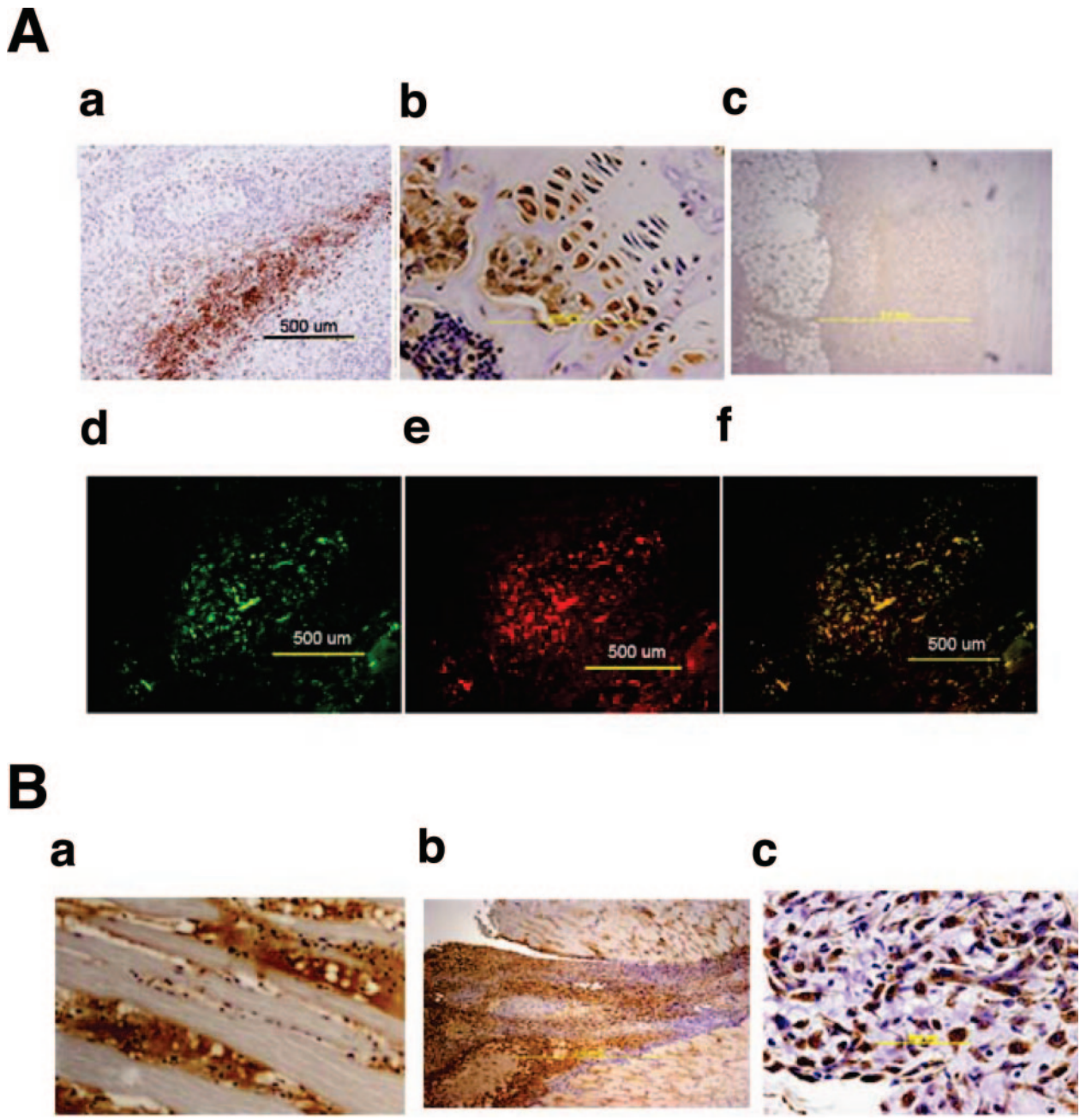

Figure 5. Brown adipocytes generate hypoxia in tissue stimulated with BMP2. NOD/SCID mice were injected with BMP2-producing cells as described in Materials and Methods. **A:** Hypoxic regions appear in and near the site of injection. On day 3, mice were injected with pimonidazole, which was subsequently detected with an antibody against this compound (Hypoxyprobe monoclonal antibody). One of the hypoxic regions is shown in **a**. **b:** The growth plate of an uninfected NOD/SCID mouse processed similarly, and **c:** the lack of staining in the same region in a mouse 3 days after injection of cells transduced with control virus Ad5F35-null. Sections obtained at day 3 and embedded in paraffin were double-labeled with antibodies against pimonidazole (Hypoxyprobe; **d**, green) and PGC-1α (**e**, red). **f:** A merger of **d** and **e**. **B: a:** The close correlation between positive staining with the Hypoxyprobe monoclonal antibody (brown) and brown adipocytes 1 day after injection of BMP2-producing cells; **b:** a large portion of the area of the lesion is hypoxic 4 days of injection of BMP2-producing cells. **c:** Significant staining of cells in the area of injection for HIF-1, 2 days after injection. Original magnifications: ×10.5 (**A**, **Bc**); ×20.5 (**Ba**); ×4.5 (**Bb**).

Misty Mice Show an Excessive Accumulation of Heterotopic Bone

If brown adipocytes do in fact support the early formation of ectopic bone, injection of *misty* mice with BMP2-expressing cells should either fail to generate bone or perhaps stimulate aberrant bone formation through a compensatory mechanism. We therefore studied BMP2-treated *misty* and C57BL/6 mice at 3, 4, and 6 days after injection (n = 5 mice per time point). In contrast to findings in the latter group, there were no brown adipocytes interspersed among the muscle fibers in the injection site in *misty* mice on day 3 (Figure 7, top). Unexpectedly, the white adipocytes pre-existing in the injection site in *misty*, but not those in C57BL/6, mice were drastically reduced in size on days 3, 4, and 6 (Figure 7). This result

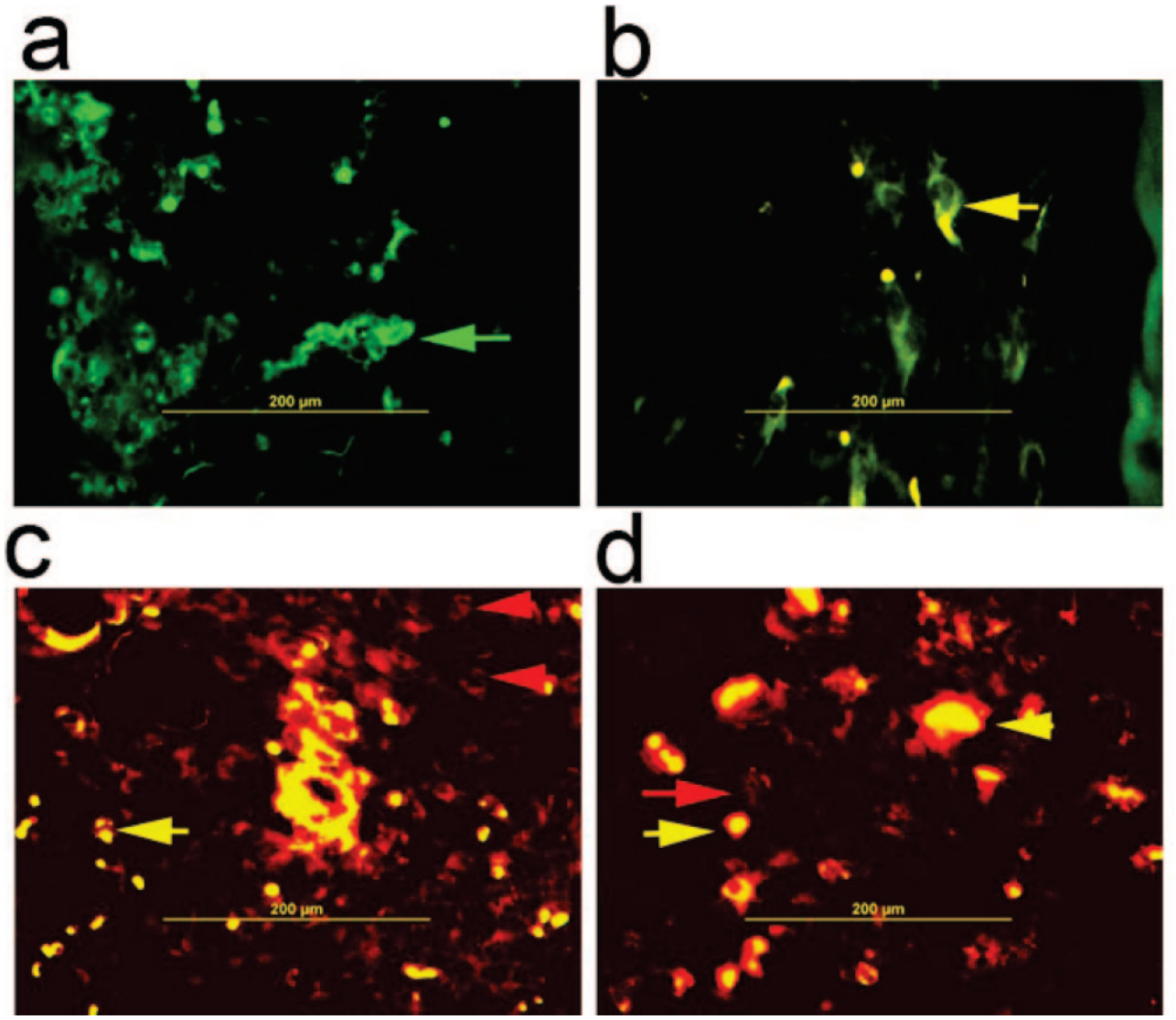

Figure 6. Kinetics of UCP-1 synthesis in relation to hypoxia. Sections obtained either 1 (**a**), 2 (**b**), 4 (**c**), or 5 (**d**) days after injection of BMP2-producing cells were stained with a mixture of Hypoxyprobe mouse monoclonal antibody (red color) and a rabbit polyclonal antibody against UCP-1 (green color). Antibody binding was detected by incubation of the stained section with Qdot 525 goat $F(ab')_2$ anti-rabbit IgG conjugate (red) and Q-dot 565 goat $F(ab')_2$ anti-mouse IgG conjugate (green). **Green arrows**, cells expressing UCP-1; **red arrows**, hypoxic cells not expressing UCP-1; **yellow arrows**, hypoxic cells expressing UCP-1. Original magnifications, ×20.5.

indicates that BMP2 stimulation had induced oxidative metabolism in these white adipocytes, indicated by their loss of fat globules (Figure 7), analogous to the conversion of white adipocytes to fat-oxidizing machines after treatment with leptin.[34]

The widespread oxidation of white fat in *misty* mice seems to have created a larger hypoxic region than seen in conventional mice, leading to increased cartilage formation and ultimately enhanced bone development. To test this idea, we injected both C57BL/6 and *misty* mice with pimonidazole 3 days after the injection of BMP2-expressing cells. Comparison of histological sections at this interval showed hypoxic areas of brown but not white fat in C57BL/6 mice (Figure 8, compare c and e), whereas in *misty* mice the white fat cells were clearly hypoxic (Figure 8f). However, neither the white fat of C57BL/6 mice (Figure 8e) nor the region of cell injection in *misty* mice (Figure 8d) was hypoxic. We calculated the volumes of the hypoxic areas in both *misty* and C57BL/6 mice using histomorphometry ($n = 3$). The volume of the hypoxic region in *misty* mice was 359 ± 39 μm^3 compared with 134 ± 21 μm^3 in C57BL/6 mice ($P = 0.002$). Therefore, the *misty* mice had 2.7 times more hypoxic regions than the C57BL/6 mice.

To determine whether hypoxic conversion of white adipocytes in the *misty* mouse results in greater bone production, we injected either *misty* ($n = 6$) or C57BL/6 ($n = 6$) mice with BMP2-expressing cells. After 14 days, all animals were euthanized, and tissue from each animal was examined by micro-CT. Figure 9, a and b, presents the tomographic results with a statistical comparison of bone formation. The mean volume of mineralized tissue (heterotopic bone) in *misty* mice was 3.4-fold greater than that in C57BL/6 (Figure 9b, $P = 0.002$). This result was

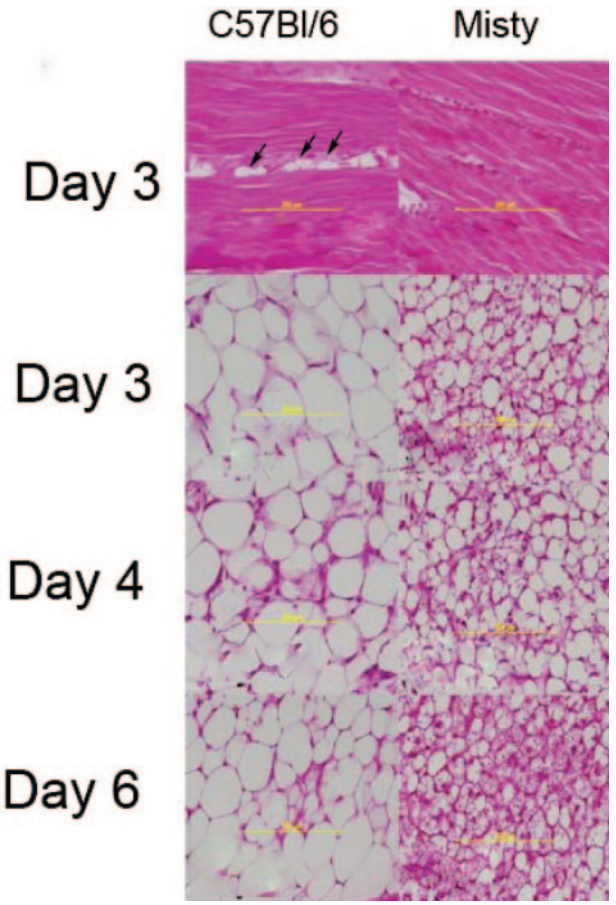

Figure 7. Analysis of fat burning in *misty* mice that lack brown fat. BMP2-producing MC3T3 cells were injected into *misty* ($n = 5$) and C57BL/6 mice ($n = 5$), and tissue samples were examined for brown adipocytes on days 3, 4, and 6. Top left and right panels show the presence (C57BL/6) and absence (*misty*) of brown adipocytes between muscle fibers.

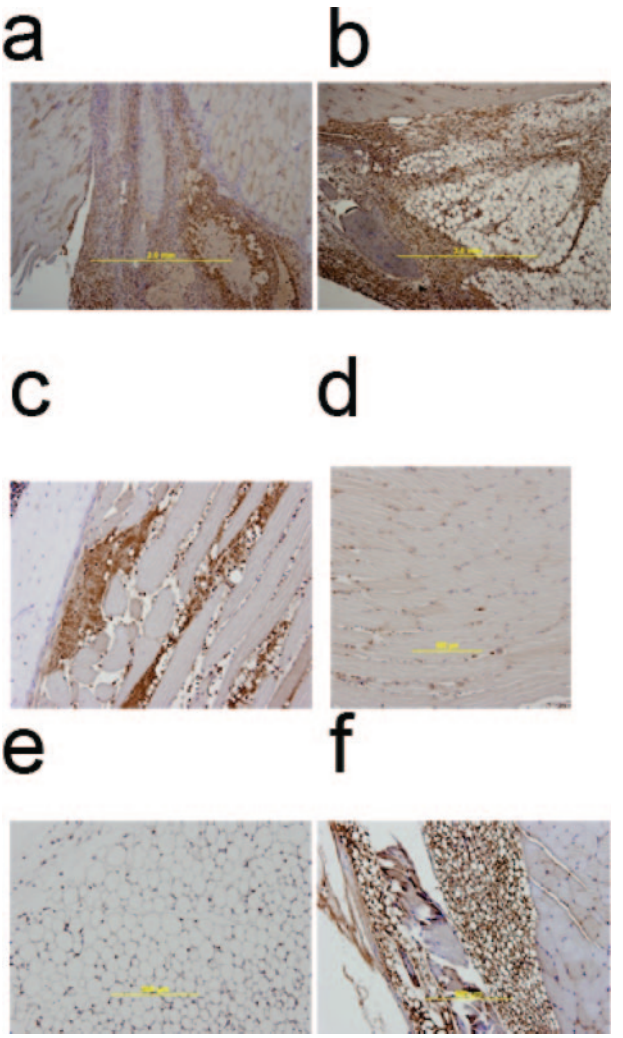

Figure 8. Analysis of hypoxia in *misty* and C57BL/6 mice. Subgroups of the mice described in Figure 7 were injected with pimonidazole at 3 days after injection and euthanized, and their limbs were prepared for staining with Hypoxyprobe. **a:** Day 4; **c**, day 3; and **e**, day 4; for C57BL/6 mice. **b:** Day 4; **d**, day 3; and **f**, day 4; for *misty* mice. Brown staining corresponds to areas of hypoxia.

predicted from the histological sections of heterotopic bone observed at 14 days from *misty* (Figure 9c, top) and C57BL/6 (Figure 9c, bottom) and confirmed by static histomorphometry an example of which is shown in Figure 9d. The volume of osteoid was 132.6 ± 61.8 μm^3 for the *misty* mice and 24.0 ± 9.9 μm^3 for the C57BL/6 mice ($n = 4$, $P \leq 0.001$). Therefore, by this method the volume of osteoid was 5.5-fold greater in the *misty* mouse than in C57BL/6 mice. We assume that increased hypoxia induction in *misty* mouse described above leads to increased chondrogenesis that ultimately leads to increased bone formation.

Finally, to give further credence to the concept that white adipocytes are used as a compensatory mechanism when brown adipocytes are unavailable, we measured the numbers of total adipocytes in the lesional area surrounding the injection site 3 days after injection of BMP2-producing cells in C57BL/6 and *misty* mice. Table 1 presents these data, which show that there were 3.5 times more adipocytes in the region surrounding the site of injection in *misty* compared with C57BL/6 mice.

Discussion

In these studies, we investigated the microenvironmental factors that might be conducive to osteogenesis, using an experimental model of BMP2-induced heterotopic ossification, and found that the induction of hypoxia by brown adipocytes is an early event in this process. Although brown and white adipocytes express many of the same adipocyte-specific genes,[29] they have distinctly different functions. The primary role of white adipocytes is to store excess energy as lipid, whereas brown adipocytes have the exclusive role of converting food and oxygen into heat, a process mediated by UCP-1. Once activated, UCP-1 uncouples mitochondrial respiration from ATP synthesis, leading to the dissipation of energy in the form of heat. Classically, this reaction is thought to occur only when the organism requires extra heat, as in arousal from hibernation or immediately after birth. Thus, it is not surprising that healthy human children and adults,

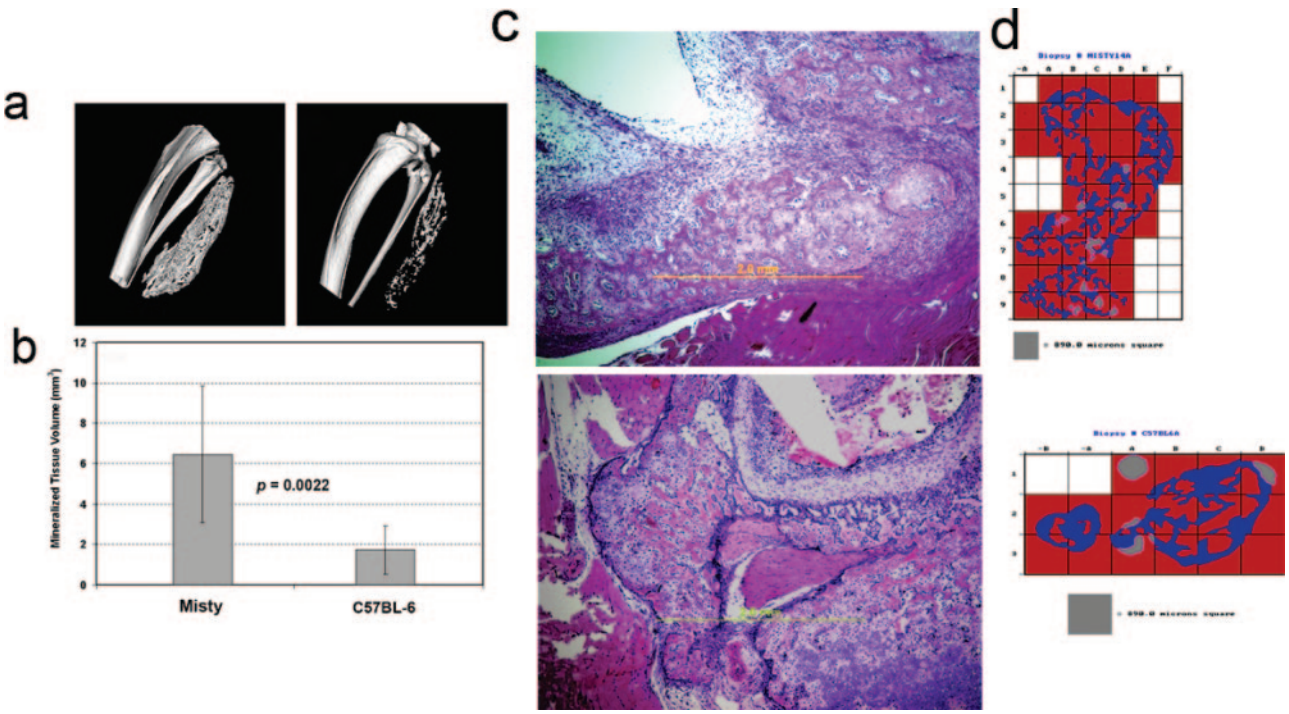

Figure 9. Morphometric analysis of bone formation in *misty* and C57BL/6 mice. **a** and **b:** Micro-CT analysis of the bone formed at 14 days after injection with BMP2-producing MC3T3 cells in *misty* and C57BL/6 mice, with comparison of mineralized tissue volumes. **c:** Histology (H&E) of sections of bone in *misty* (top) and C57BL/6 mice. **d:** Example of sections analyzed by histomorphometry, (*misty*, top).

who are primarily protected from extreme cold, lack appreciable depots of functional brown fat.[29] However, despite its reputation as a vestigial organ in humans, brown adipose tissue has the capacity for oxidative metabolism with minimal generation of free radicals[35] and thus is ideally suited for physiological or pathological processes that require hypoxic conditions.

We used several criteria to identify brown adipocytes in our model of heterotopic ossification: 1) characteristic morphology (multiple lipid droplets and a high number of mitochondria in particular); 2) expression of the definitive brown adipocyte marker UCP-1; 3) the absence of UCP-1-positive cells in *misty* mice; and 4) expression of PGC-1α, a PPAR-γ-interacting protein expressed preferentially in brown compared with white adipocytes.[31] The accumulation of brown adipocytes in tissue stimulated with BMP2 places these cells in a unique position to orchestrate heterotopic ossification through the regulation of oxygen tension in the local microenvironment. The depletion of tissue oxygen stores through uncoupled mitochondrial respiration would be expected to induce chondrocyte-specific gene expression in mesenchymal stem cells, leading to differentiation of the stem cells to mature chondrocytes.[30]

Table 1. Distribution of Adipocytes on Day 3 in the Region of Heterotopic Bone Formation

Mice	Adipocytes per section per mouse	
	Misty	C57BL/6
Mouse 1	46,527	10,352
Mouse 2	71,906	27,205
Mouse 3	101,894	24,903
Mouse 4	80,206	21,200
Average adipocytes per section per mouse	75,133 ± 13,037	20,915 ± 7464

MC3T3 cells transduced using Ad5BMP2 were injected into the quadriceps of either *Misty* or C57BL/6 mice (n = 4) using procedures described in Materials and Methods. On the 3rd day after injection, mice were euthanized, and paraffin sections were prepared from the muscle around the site of injection. After H&E staining of sections, adipocytes were counted (10 sections per mouse, four mice per group) with the aid of FOVEA Pro 4.0 plug-ins (Reindeer Graphics, Asheville, NC) for Adobe Photoshop from the region either in or immediately adjacent to the area of heterotopic bone formation. The ratio of *Misty*:C57BL/6 is 3.6, and the average number of adipocytes per section per mouse is presented above. P = 0.013.

In animals lacking brown adipocytes, the volume of the bone formed in response to BMP2 stimulation was nearly triple that in animals with normal production of brown adipose tissue (Figure 9) when evaluated by micro-CT and more than fivefold greater when evaluated by static histomorphometry. The quantitative discrepancy between micro-CT and histomorphometry has been observed before.[36] Both methods of evaluation agree qualitatively, suggesting that an alternative cell may also be capable of inducing hypoxia. We propose that brown fat is preferentially used to generate hypoxic stress during heterotopic bone formation. If such cells are not available, white fat near the site of BMP2 synthesis is burned, analogous to the oxidative destruction of this tissue after treatment with leptin.[34] This process creates large hypoxic areas (Figure 5) as a microenvironment for cartilage formation. This hypothesis gains support from reports of a link between BMP expression and fatty acid metabolism in adipocytes.[37] It also gains credence when one notes the close correlation between the amount of

excess bone formed in mice lacking brown fat and the ratio of the white to brown adipocytes in the immediate area surrounding the site of injection (Table 1).

The relevancy of our model may extend beyond the formation of heterotopic bone in soft tissues. Fractures heal by a combination of intramembranous and endochondral types of bone generation.[38] Endochondral ossification in bone repair is very similar if not identical to the heterotopic ossification we describe; both processes include an initial stage of inflammation, followed by angiogenesis and the formation of cartilage, cartilage calcification, cartilage removal, bone formation, and ultimately bone remodeling.[38] It is also know that BMPs are intimately involved in fracture healing.[39] If brown adipocytes participate in fracture repair, as we suspect, our heterotopic ossification model should prove useful in devising methods to enhance new bone formation at the fracture site.

BMPs can drive the differentiation of mesenchymal stem cells toward the adipocyte, chondrocyte, or osteoblast lineage, depending on the transcriptional mechanisms that are activated.[40] Thus, the very early appearance of brown adipocytes in our model probably stems from up-regulation of the PPAR-γ pathway by BMP2, followed by norepinephrine-driven expression of PPAR-γ co-activator 1α, which seems to mediate the conversion of these cells to brown adipocytes.[31] This would imply an initial effect of BMP2 on sympathetic neurons or their progenitors, similar to that described[41] on neural crest progenitors to induce their differentiation. Indeed, BMP receptors are present on sympathetic neurons,[42,43] and BMP produced in the dorsal aorta is sufficient to induce noradrenergic differentiation,[44,45] whereas its blockade by noggin prevents the expression of noradrenergic and pan-neuronal properties.[46] BMP2 can also elicit the production of neurotrophic factors such as glial-derived neurotrophic factor,[47] which could cause neurite outgrowth into the injected area.[48] On the other hand, BMP could independently induce adipocyte differentiation in our model, and there is precedent for BMP involvement in the induction of adipogenesis.[49,50]

Other targets of BMP2 action in our heterotopic ossification model are less clear, although several BMP-activated signaling pathways are critical in the regulation of chondrogenesis.[51] Early in this process, BMPs are required to maintain *Sox* gene expression and continuous BMP stimulation is needed to complete chondrocyte differentiation.[52–54] These proteins exert their essential regulatory roles via effects on the Indian hedgehog/parathyroid hormone-related protein and fibroblast growth factor pathways.[51] The precise contributions of BMP2 to the signaling cascades that drive heterotopic ossification in our model remain to be determined.

The term heterotopic ossification refers to a number of pathological processes that have the formation of bone in soft tissue as an end point.[1] Although the exact relationship of our model to each category of heterotopic bone formation is uncertain, we suggest that BMP-induced generation of brown adipocytes may be a common event in these diverse processes. Thus, further studies are planned to test whether elimination of hypoxic stress would block bone formation in muscle. This approach to therapy would be analogous to the use of anti-angiogenic agents to inhibit new blood vessel formation to slow or inhibit the subsequent production of heterotopic bone[6]

Acknowledgments

We thank John Gilbert for editing the manuscript and Scott Vacha (Agilent Technologies, Palo Alto, CA) for assistance with the microarray analysis.

References

1. Kaplan FS, Glaser DL, Hebela N, Shore EM: Heterotopic ossification. J Am Acad Orthop Surg 2004, 12:116–125
2. Kaplan FS, Shore EM, Connor JM: Fibrodysplasia ossificans progressiva. Connective Tissue and its Heritable Disorders: Molecular, Genetic, and Medical Aspects., ed 2. Edited by PM Royce, B Steinman. Wilmington, DE, Wiley-Liss, 2002, p 827
3. Shore EM, Xu M, Feldman GJ, Fenstermacher DA, Brown MA, Kaplan FS: A recurrent mutation in the BMP type I receptor ACVR1 causes inherited and sporadic fibrodysplasia ossificans progressiva. Nat Genet 2006, 38:525–527
4. Mohler III ER, Gannon F, Reynolds C, Zimmerman R, Keane MG, Kaplan FS: Bone formation and inflammation in cardiac valves. Circulation 2001, 103:1522–1528
5. Ahn J, Serrano de la Pena L, Shore EM, Kaplan FS: Paresis of a bone morphogenetic protein-antagonist response in a genetic disorder of heterotopic skeletogenesis. J Bone Joint Surg Am 2003, 85A:667–674
6. Yin M, Gentili C, Koyama E, Zasloff M, Pacifici M: Antiangiogenic treatment delays chondrocyte maturation and bone formation during limb skeletogenesis. J Bone Miner Res 2002, 17:56–65
7. Schipani E, Ryan HE, Didrickson S, Kobayashi T, Knight M, Johnson RS: Hypoxia in cartilage: HIF-1alpha is essential for chondrocyte growth arrest and survival. Genes Dev 2001, 15:2865–2876
8. Pfander D, Cramer T, Schipani E, Johnson RS: HIF-1alpha controls extracellular matrix synthesis by epiphyseal chondrocytes. J Cell Sci 2003, 116:1819–1826
9. Mobasheri A, Richardson S, Mobasheri R, Shakibaei M, Hoyland JA: Hypoxia inducible factor-1 and facilitative glucose transporters GLUT1 and GLUT3: putative molecular components of the oxygen and glucose sensing apparatus in articular chondrocytes. Histol Histopathol 2005, 20:1327–1338
10. Urist MR, Nakagawa M, Nakata N, Nogami H: Experimental myositis ossificans: cartilage and bone formation in muscle in response to a diffusible bone matrix-derived morphogen. Arch Pathol Lab Med 1978, 102:312–316
11. Olmsted-Davis EA, Gugala Z, Gannon FH, Yotnda P, McAlhany RE, Lindsey RW, Davis AR: Use of a chimeric adenovirus vector enhances BMP2 production and bone formation. Hum Gene Ther 2002, 13:1337–1347
12. Gugala Z, Olmsted-Davis EA, Gannon FH, Lindsey RW, Davis AR: Osteoinduction by ex vivo adenovirus-mediated BMP2 delivery is independent of cell type. Gene Ther 2003, 10:1289–1296
13. Olmsted EA, Blum JS, Rill D, Yotnda P, Gugala Z, Lindsey RW, Davis AR: Adenovirus-mediated BMP2 expression in human bone marrow stromal cells. J Cell Biochem 2001, 82:11–21
14. Fouletier-Dilling CM, Bosch P, Davis AR, Shafer JA, Stice SL, Gugala Z, Gannon FH, Olmsted-Davis EA: Novel compound enables high-level adenovirus transduction in the absence of an adenovirus-specific receptor. Hum Gene Ther 2005, 16:1287–1297
15. Southwood LL, Frisbie DD, Kawcak CE, McIlwraith CW: Delivery of growth factors using gene therapy to enhance bone healing. Vet Surg 2004, 33:565–578
16. Khan SN, Lane JM: The use of recombinant human bone morphogenetic protein-2 (rhBMP-2) in orthopaedic applications. Expert Opin Biol Ther 2004, 4:741–748
17. Shafritz AB, Shore EM, Gannon FH, Zasloff MA, Taub R, Muenke M,

Kaplan FS: Overexpression of an osteogenic morphogen in fibrodysplasia ossificans progressiva. N Engl J Med 1996, 335:555–561
18. Zhao GQ: Consequences of knocking out BMP signaling in the mouse. Genesis 2003, 35:43–56
19. Cao B, Huard J: Muscle-derived stem cells. Cell Cycle 2004, 3:104–107
20. Olmsted-Davis EA, Gugala Z, Camargo F, Gannon FH, Jackson K, Kienstra KA, Shine HD, Lindsey RW, Hirschi KK, Goodell MA, Brenner MK, Davis AR: Primitive adult hematopoietic stem cells can function as osteoblast precursors. Proc Natl Acad Sci USA 2003, 100:15877–15882
21. Dominici M, Pritchard C, Garlits JE, Hofmann TJ, Persons DA, Horwitz EM: Hematopoietic cells and osteoblasts are derived from a common marrow progenitor after bone marrow transplantation. Proc Natl Acad Sci USA 2004, 101:11761–11766
22. Verfaillie CM: Multipotent adult progenitor cells: an update. Novartis Found Symp 2005, 265:55–61
23. Sviderskaya EV, Novak EK, Swank RT, Bennett DC: The murine misty mutation: phenotypic effects on melanocytes, platelets and brown fat. Genetics 1998, 148:381–390
24. Manual of Histologic Staining Methods of the Armed Forces Institute of Pathology., ed 3. Edited by L Luna. New York, McGraw Hill, 1968
25. Parfitt AM, Drezner MK, Glorieux FH, Kanis JA, Malluche H, Meunier PJ, Ott SM, Recker RR: Bone histomorphometry: standardization of nomenclature, symbols, and units. Report of the ASBMR Histomorphometry Nomenclature Committee. J Bone Miner Res 1987, 2:595–610
26. Zheng MH, King E, Kirilak Y, Huang L, Papadimitriou JM, Wood DJ, Xu J: Molecular characterisation of chondrocytes in autologous chondrocyte implantation. Int J Mol Med 2004, 13:623–628
27. Sell H, Deshaies Y, Richard D: The brown adipocyte: update on its metabolic role. Int J Biochem Cell Biol 2004, 36:2098–2104
28. Nedergaard J, Golozoubova V, Matthias A, Asadi A, Jacobsson A, Cannon B: UCP1: the only protein able to mediate adaptive nonshivering thermogenesis and metabolic inefficiency. Biochim Biophys Acta 2001, 1504:82–106
29. Cannon B, Nedergaard J: Brown adipose tissue: function and physiological significance. Physiol Rev 2004, 84:277–359
30. Robins JC, Akeno N, Mukherjee A, Dalal RR, Aronow BJ, Koopman P, Clemens TL: Hypoxia induces chondrocyte-specific gene expression in mesenchymal cells in association with transcriptional activation of Sox9. Bone 2005, 37:313–322
31. Puigserver P, Spiegelman BM: Peroxisome proliferator-activated receptor-gamma coactivator 1 alpha (PGC-1 alpha): transcriptional coactivator and metabolic regulator. Endocr Rev 2003, 24:78–90
32. Semenza GL: Oxygen-regulated transcription factors and their role in pulmonary disease. Respir Res 2000, 1:159–162
33. Li B, Holloszy JO, Semenkovich CF: Respiratory uncoupling induces delta-aminolevulinate synthase expression through a nuclear respiratory factor-1-dependent mechanism in HeLa cells. J Biol Chem 1999, 274:17534–17540
34. Orci L, Cook WS, Ravazzola M, Wang MY, Park BH, Montesano R, Unger RH: Rapid transformation of white adipocytes into fat-oxidizing machines. Proc Natl Acad Sci USA 2004, 101:2058–2063
35. Brand MD, Buckingham JA, Esteves TC, Green K, Lambert AJ, Miwa S, Murphy MP, Pakay JL, Talbot DA, Echtay KS: Mitochondrial superoxide and aging: uncoupling-protein activity and superoxide production. Biochem Soc Symp 2004, (71):203–213
36. Chappard D, Retailleau-Gaborit N, Legrand E, Basle MF, Audran M: Comparison insight bone measurements by histomorphometry and microCT. J Bone Miner Res 2005, 20:1177–1184
37. Witthuhn BA, Bernlohr DA: Upregulation of bone morphogenetic protein GDF-3/Vgr-2 expression in adipose tissue of FABP4/aP2 null mice. Cytokine 2001, 14:129–135
38. Einhorn TA: The cell and molecular biology of fracture healing. Clin Orthop Relat Res 1998, (355 Suppl):S7–21
39. Dimitriou R, Tsiridis E, Giannoudis PV: Current concepts of molecular aspects of bone healing. Injury 2005, 36:1392–1404
40. Miyazono K, Maeda S, Imamura T: BMP receptor signaling: transcriptional targets, regulation of signals, and signaling cross-talk. Cytokine Growth Factor Rev 2005, 16:251–263
41. Shah NM, Groves AK, Anderson DJ: Alternative neural crest cell fates are instructively promoted by TGFbeta superfamily members. Cell 1996, 85:331–343
42. Zhang D, Mehler MF, Song Q, Kessler JA: Development of bone morphogenetic protein receptors in the nervous system and possible roles in regulating trkC expression. J Neurosci 1998, 18:3314–3326
43. Mehler MF, Mabie PC, Zhu G, Gokhan S, Kessler JA: Developmental changes in progenitor cell responsiveness to bone morphogenetic proteins differentially modulate progressive CNS lineage fate. Dev Neurosci 2000, 22:74–85
44. Reissmann E, Ernsberger U, Francis-West PH, Rueger D, Brickell PM, Rohrer H: Involvement of bone morphogenetic protein-4 and bone morphogenetic protein-7 in the differentiation of the adrenergic phenotype in developing sympathetic neurons. Development 1996, 122:2079–2088
45. Ernsberger U: Evidence for an evolutionary conserved role of bone morphogenetic protein growth factors and phox2 transcription factors during noradrenergic differentiation of sympathetic neurons. Induction of a putative synexpression group of neurotransmitter-synthesizing enzymes. Eur J Biochem 2000, 267:6976–6981
46. Schneider C, Wicht H, Enderich J, Wegner M, Rohrer H: Bone morphogenetic proteins are required in vivo for the generation of sympathetic neurons. Neuron 1999, 24:861–870
47. Kinameri E, Matsuoka I: Autocrine action of BMP2 regulates expression of GDNF-mRNA in sciatic Schwann cells. Brain Res Mol Brain Res 2003, 117:221–227
48. Hashino E, Shero M, Junghans D, Rohrer H, Milbrandt J, Johnson Jr EM: GDNF and neurturin are target-derived factors essential for cranial parasympathetic neuron development. Development 2001, 128:3773–3782
49. Sottile V, Seuwen K: Bone morphogenetic protein-2 stimulates adipogenic differentiation of mesenchymal precursor cells in synergy with BRL 49653 (rosiglitazone). FEBS Lett 2000, 475:201–204
50. Jin W, Takagi T, Kanesashi SN, Kurahashi T, Nomura T, Harada J, Ishii S: Schnurri-2 controls BMP-dependent adipogenesis via interaction with Smad proteins. Dev Cell 2006, 10:461–471
51. Yoon BS, Lyons KM: Multiple functions of BMPs in chondrogenesis. J Cell Biochem 2004, 93:93–103
52. Shukunami C, Ohta Y, Sakuda M, Hiraki Y: Sequential progression of the differentiation program by bone morphogenetic protein-2 in chondrogenic cell line ATDC5. Exp Cell Res 1998, 241:1–11
53. Ito H, Akiyama H, Shigeno C, Nakamura T: Noggin and bone morphogenetic protein-4 coordinately regulate the progression of chondrogenic differentiation in mouse clonal EC cells, ATDC5. Biochem Biophys Res Commun 1999, 260:240–244
54. Shukunami C, Akiyama H, Nakamura T, Hiraki Y: Requirement of autocrine signaling by bone morphogenetic protein-4 for chondrogenic differentiation of ATDC5 cells. FEBS Lett 2000, 469:83–87